

Effects of Cooperative Adaptive Cruise Control on Traffic Flow Stability

Wouter J. Schakel, Bart van Arem, *Member, IEEE*, and Bart D. Netten

Abstract—The effects of Cooperative Adaptive Cruise Control (CACC) on traffic flow is an important issue as traffic flow stability, capacity and safety are concerned. In contrast to most research we focus on traffic flow stability. We use the Intelligent Driver Model and CACC algorithms to assess the effects. A recently field-tested and CACC-based advisory system is also evaluated as an intermediate solution. It is found that CACC can quickly damp shockwaves at lower penetration rates (50%) and that shockwaves move faster.

I. INTRODUCTION

TRAFFIC all over the world suffers from congestion. Congestion starts as shockwaves in which drivers are forced to decelerate. Shockwaves may grow in length and even in width (lane synchronization). However, shockwaves may also be ‘absorbed’ in traffic. Usually these shockwaves are referred to as unstable and stable traffic respectively. A more comprehensive description of stability can be found in [1], where a distinction between local, platoon and traffic flow stability is made. Shockwaves have many drawbacks related to fuel consumption, the environment, travel time, and traffic safety. As shockwaves have no merits, many attempts have been made to reduce or prevent them.

Advanced Driver Assistance systems aim at helping the driver with various tasks related to the driving task such as lane keeping and collision avoidance. One of the most common Advanced Driver Assistance systems is Adaptive Cruise Control. Adaptive Cruise Control tries to maintain a certain speed and is able to follow a slower predecessor. More advanced Adaptive Cruise Control systems also use communication between vehicles. This type of Adaptive Cruise Control is called Cooperative Adaptive Cruise Control or CACC. It results in more stable traffic than Adaptive Cruise Control. We focus on CACC systems that communicate with multiple vehicles ahead. This concept is relatively new and only little research has been performed on this subject. CACC systems are able, similarly to humans, to ‘look’ further ahead than one vehicle and to anticipate

accordingly. CACC systems can perform this task better than humans as anticipation can be performed for more vehicles and because speed differences, distances and acceleration are estimated more precisely. Also the response time of CACC is much lower compared to human drivers. Potentially these systems reduce all the downsides that come with shockwaves, though into different extents.

An Acceleration Advise Control (AAC) system is an advisory system based on a CACC. It uses the CACC to give an acceleration advice enabling a driver to anticipate more accurately and well in advance of disturbances further ahead. An AAC algorithm is evaluated here and compared to the results of a recently held large Field Operational Test [2].

In this article we investigate into what extent a realistic CACC algorithm is indeed able to mitigate shockwaves. Shockwave characteristics are evaluated for different levels of CACC penetration. From these characteristics some plausible hypotheses are made on the implications for human drivers in mixed traffic and the effectiveness of CACC. Generally shockwaves are damped quicker with higher penetrations of CACC.

In section 2 it is described what car-following model for human drivers is most suitable for comparison with CACC systems. Section 3 describes CACC systems and the existing knowledge. Next, section 4 gives results of a large Field Operational Test. Sections 5 and 6 describe a modeling framework for CACC and present the results. Sections 7 and 8 finally give some discussion and conclusions.

II. MODELING HUMAN DRIVERS

A. Car-following models

In microscopic traffic flow models the so-called longitudinal driving task is modeled using a combination of free flow driving and car-following models. For decades attempts have been made to capture human driver behavior in a car-following model. A representation of human behavior regarding traffic flow stability should have realistic shockwave patterns and macroscopic capacity. To this end we have looked at several car-following models.

The Intelligent Driver Model (IDM) is presented in [3]. The main feature of the model is the non-linear response to speed differences, included in s^* , the dynamic desired headway. The acceleration is determined in (1).

Manuscript received April 12, 2010. This work was supported by the SPITS project (<http://spits-project.com>).

W. J. Schakel is PhD at the Delft University of Technology, department of transport and planning (corresponding author, phone: +31 (0)15 278 4030, e-mail: W.J.Schakel@tudelft.nl).

B. van Arem is professor at the Delft University of Technology, department of transport and planning (phone: +31 (0)15 278 6342, e-mail: B.vanArem@tudelft.nl).

B.D. Netten is senior researcher at TNO (phone: +31 (0)15 269 2059, e-mail: bart.netten@tno.nl).

$$\frac{dv}{dt} = a \cdot \left[1 - \left(\frac{v}{v_0} \right)^4 - \left(\frac{s^*(v, \Delta v)}{s} \right)^2 \right] \quad (1)$$

with,

$$s^*(v, \Delta v) = s_0 + vT + \frac{v\Delta v}{2\sqrt{ab}} \quad (2)$$

where a is the comfortable acceleration, v is the current speed, v_0 is the desired speed, s_0 is the minimum headway (at standstill), T is the desired time headway, Δv is the speed difference with the leader, s is the current distance headway and b is the comfortable deceleration. The IDM shows realistic shockwave patterns but has a macroscopic capacity of just below 1900 veh/h, see figure 1a. In order to reach a reasonable capacity, the desired time headway needs to be lowered to unreasonable values.

We have also looked at the Optimal Velocity Model [4]. In the Optimal Velocity Model the acceleration is determined by adapting the speed to a desired speed with a certain relaxation. The desired speed is dependant on the free flow desired speed and the headway. The Optimal Velocity Model is not always collision free and performs worse than the IDM in representing trajectory data [5].

Another frequently used car-following model is the model by Helly [6], and the many variations to this model. These models are straight forward and easy to understand. However, the linear responses to deviation from desired headway and desired speed do not result in realistic shockwave patterns. We have tested the model and found that shockwaves grow, that is, the region where speeds are lower grows both backwards and slightly forwards while the lowered speed remains constant. This is a-typical behavior for congestion.

B. Selected car-following model

As we are focusing on traffic flow stability we have chosen to use an adapted version of the IDM, here referred to as IDM+. We have adapted the IDM to achieve reasonable capacity values. To this end we apply a minimization over the free-flow and the interaction terms of (1), similarly to models based on Helly and Gipps [7].

$$\frac{dv}{dt} = a \cdot \min \left[1 - \left(\frac{v}{v_0} \right)^4, 1 - \left(\frac{s^*(v, \Delta v)}{s} \right)^2 \right] \quad (3)$$

By explicitly separating the free-flow and interaction terms, the equilibrium fundamental diagram of the IDM changes from a smooth topped-off shape to a triangular shape as in figure 1a. For $v/v_0 < 1$ or $s^*/s < 1$ (region A+B+C in figure 1b) the acceleration difference is small. The figure is normalized with respect to parameter a thus the acceleration difference in this region is smaller than a . Note

that this contains the region of normal operations as drivers will have $v_0 \geq v$ (region B+C) on a homogenous stretch of road. Drivers also have $s > s^*$ (region A+B) in free flow conditions and $s \approx s^*$ in congested conditions. Unstable behavior in the IDM is largely dependant on s^* as this includes the exaggerated response to speed difference and deviation from the equilibrium headway. Strong decelerations triggering traffic flow instability occur with $s^* \gg s$. This still holds for the IDM+ as long as $v \leq v_0$ (region C instead of D). The maximum acceleration difference is then equal to a .

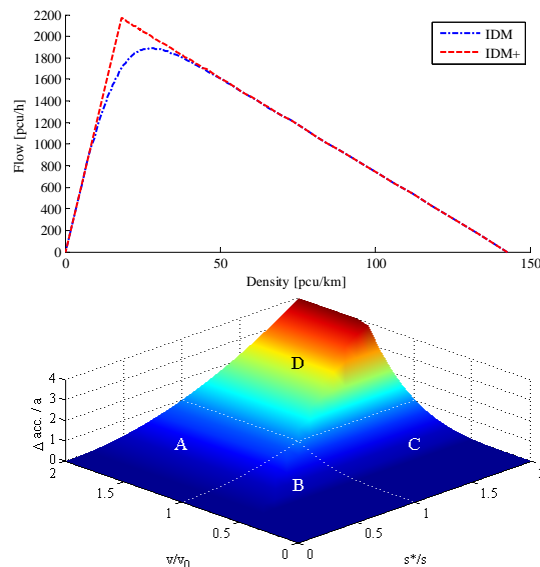


Fig. 1. (a) Equilibrium fundamental diagram of the IDM and IDM+ with $v_0 = 120$ km/h, $s_0 = 2$ m, $T = 1.45$ s and a vehicle length of 5 m. For the IDM the equilibrium gap is calculated as in [3]. For the IDM+ an equilibrium gap of $s_0 + vT$ is used. From the equilibrium gap a density can be derived using the vehicle length. Multiplying with v gives the flow. (b) Difference in acceleration between IDM and IDM+ (IDM+ minus IDM) normalized to parameter a . Note that all other IDM parameters are captured within the fractions v/v_0 and s^*/s . For regions A, B, and C there is little difference. Region B represents normal operations ($s \geq s^*$ & $v \leq v_0$).

III. ADVANCED DRIVER ASSISTANCE SYSTEMS AND MODELS

Much research into the effects of Adaptive Cruise Control systems has been performed. For instance in [8] the IDM is adapted to a less over reactive version. Next the Adaptive Cruise Control settings are made dynamic depending on the situation (free traffic, upstream front, congested traffic, downstream front, bottleneck). The main impact found was an increased capacity.

Present research has focused mainly on throughput and comfort. We however focus mainly on traffic flow stability and investigate implications for human drivers in mixed traffic. In the Netherlands TNO has developed and tested CACC systems that are the basis of our research.

A. IRSA Controller

In [9] the Integrated full-Range Speed Assistant (or IRSA) controller was evaluated. IRSA is a CACC system as described in [10]. Positive effects on capacity and comfort were found. In [11] MIXIC 1.3 [12] was used to evaluate the effects of a dedicated lane for CACC vehicles. Again positive effects on capacity were found although the lane changing process was made more difficult because of platoons with vehicles closely following each other.

The IRSA controller has multiple versions. We have used the CACC2 as this is applicable even when not all vehicles are equipped. This allows investigation into the effects at multiple penetration rates. An important building block in the IRSA controller is a regular Adaptive Cruise Control. The Adaptive Cruise Control acceleration of vehicle d is defined in (4).

$$a_d = \min(k_{cc}(v_{cc} - v_x), k_2 e_v + k_1 e_x) \quad (4)$$

Here k_{cc} is a constant gain, v_{cc} is the desired speed, v_x is the vehicle velocity, e_v is the relative speed error (downstream vehicle speed minus v_x), e_x is the relative distance error and k_1 and k_2 are non-linear gains. The CACC2 version of the IRSA controller extends this control law by including the speed differences with additional leaders. Here, only equipped vehicles are included with a maximum distance of 200m to the concerned vehicle. A maximum of $n = 5$ leaders is used in (5). As CACC2 also operates with mixed traffic a relation to the distance headway is excluded.

$$a_d = \min\left(k_{cc}(v_{cc} - v_x), k_2 e_{v,d-1} + k_1 e_{x,d-1} + \left(\frac{k_2}{n-1} \sum_{i=d-n}^{d-2} e_{v,i}\right)\right) \quad (5)$$

Undefined by the IRSA documentation are e_x (or actually the desired distance headway), k_1 and k_2 . For this we use the form and few parameters from MIXIC. The desired headway is given by $x_d = c_1 + c_2 v_x + c_3 v_x^2$. Here we use $c_1 = 3$ for the minimum headway (as in MIXIC), the desired time headway for c_2 and the quadratic term is ignored giving $c_3 = 0$. In MIXIC the values of 0.3 and 1.5 are used for k_1 and k_2 respectively for the direct leader. For the remaining leaders k_2 equals 0.2. Here values of 0.3 and 1.0 are used for all leaders. It turned out that this lead to an algorithm that is not collision free. Similarly as in MIXIC it is assumed that drivers will decelerate and override the system if necessary. A minimization over acceleration from the IRSA controller (5) and the IDM+ car-following model (1) gives the final IRSA acceleration.

B. Acceleration Advice Controller

An Acceleration Advice Controller (or AAC) is an advisory system based on a CACC system. The CACC generates an acceleration advice to the driver [2] instead of

controlling throttle and brakes directly. The CACC controller is based on [13] and adjusted to deal with large time delays due to the driver responding to the HMI. In [2] the feedforward is based on the acceleration of five predecessors. The amplification of accelerations upstream in the platoon is limited. For larger time delays, i.e. ≥ 0.4 s, the controller that is based on five predecessors is more string stable compared to [13]. The AAC was designed for 100% penetration rate and is not suitable for mixed traffic.

IV. A270 FIELD TEST

The AAC system has recently been tested in a large Field Operational Test [2] on the A270 public highway, with the objective to demonstrate the potential of CACC systems to improve traffic efficiency and shockwave behavior in particular. A string of 50 AAC equipped vehicles was put through a series of experiments in which shockwaves were induced with varying speeds and decelerations. Various decelerations were performed up to -5 m/s^2 . The largest deceleration will also be simulated in this paper. A control group of 50 unequipped vehicles was put through the same experiments in the adjacent lane. The time headway of the AAC system was set at the average of the unequipped vehicles at 1.2 s. The first results in [2] can be compared to the simulation results here.

Figure 2 shows the shockwave patterns of one of the experiments from [2]. The first wave initiated around 500 m is similar to the simulation scenario defined below. The unequipped vehicles on the left experience a shockwave (dark zone) travelling with a speed of about -20 km/h (upstream). A second wave emerges almost immediately after the first travelling about $+7 \text{ km/h}$ (downstream). Both waves do not tend to damp out within the string of 50 vehicles.

The equipped vehicles (right) tend to damp out both shockwaves. It can also be observed that the first shockwave develops as a stationary wavefront.

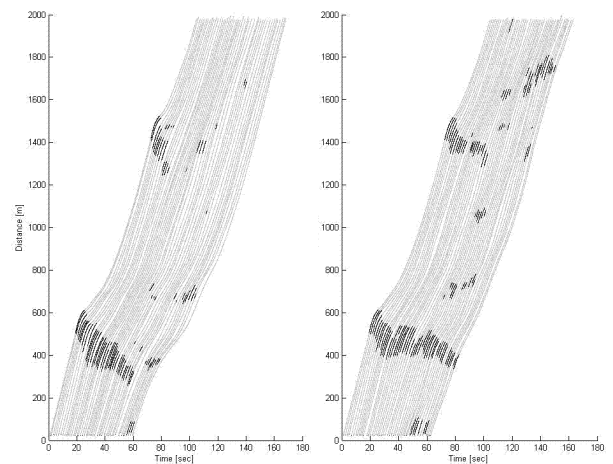


Fig. 2. Shockwave patterns from an experiment on the A270; unequipped vehicles (left), AAC equipped vehicles (right). Gray lines are vehicle trajectories (black indicates locations where vehicles decelerate with more than 1.0 m/s^2).

The conclusion from the A270 demo is that an AAC system helps drivers to better anticipate and control their decelerations and accelerations. This reduces the speed and headway variations (figure 3), and consequently stabilizes shockwaves better. Improvements of variations in traffic density of up to 13% were demonstrated.

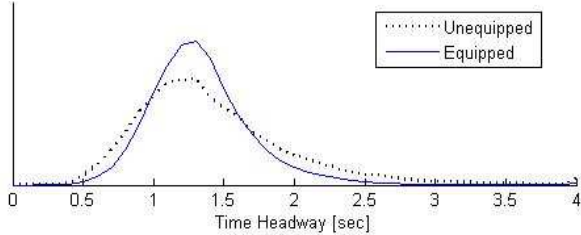


Fig. 3. Histogram of time headway over all A270 experiments; AAC equipped vehicles (continuous), unequipped vehicles (dashed).

V. SIMULATION FRAMEWORK

Human drivers and CACC equipped vehicles are simulated on a 4 km stretch of road with a single lane. The first vehicle is pre-programmed and drives at 90 km/h for the first 80 seconds covering the first 2 km. Then the vehicle decelerates at a rate of -5 m/s^2 (as in the A270 field test) to a speed of 36 km/h. This speed is maintained for 5 seconds after which the vehicle accelerates at a rate of 1 m/s^2 back to 90 km/h. As this initial perturbation forms a deceleration to 36 km/h, there is room left for shockwave growth due to unstable behavior. We have also applied a Gaussian distribution on the desired time headway both for human drivers and CACC2 equipped vehicles. This will introduce small headways that may result in unstable behavior but also large headways that may result in more stable behavior. By varying the headway standard deviation the net effect can be assessed. Note that both human drivers and CACC2 equipped vehicles have the same average desired headway as we are concerned with traffic flow stability and not with capacity, for which CACC systems can also be used.

Both the headway distribution and the CACC2 penetration have been varied. Two headway distributions have been used, 1.2 ± 0.15 seconds and 1.2 ± 0.3 seconds. The average of 1.2 seconds gives a capacity of 2400 veh/h with a desired speed of 90 km/h. The distribution of headways introduces slight decelerations at the start of the stretch of road as the vehicles are generated at a fixed headway corresponding to the inflow. This slightly decreases inflow capacity. The inflow is set at 2000 veh/h. Penetration levels of 0%, 50% and 100% have been evaluated.

The AAC algorithm of [2] is simulated in scenarios with a fixed headway and 100% penetration rate only, as the AAC algorithm is only designed for this. Driver responses to the HMI are included as a reaction time with a Gaussian distribution with an average of 0.5 s and a variation of 0.1 s. Reaction times are rounded to an integer multiple of the time step and limited at a minimum of 0.3 s.

Simulations are stopped as soon as a shockwave reaches

the start of the simulated stretch of road (collision of generated vehicle indicates spillback), after 15 minutes or as soon as all vehicles have a speed above 70 km/h after the shockwave was started (figure 4c). The applied time step is 0.1 s. Output of the simulations is in the form of vehicle trajectories. From these trajectories it can be derived whether the traffic flow reacts stable or unstable to the perturbation. Also the extent of shockwaves can be assessed.

VI. RESULTS

In order to analyze the resulting traffic flow stability the shockwave dynamics are assessed. A linear function of time is derived from the trajectories and gives the location of the shockwave. The following steps describe this derivation:

- a. For each vehicle, find the first five successive time steps with a deceleration stronger than -1 m/s^2 . This threshold is significantly larger than fluctuations with only the gas pedal (up to about -0.5 m/s^2), requiring that the brake is actually used. Decelerations on the first 100 meters are ignored as vehicles may adjust to their desired headway. The first of five time steps is the anchor point (x, t) of the shockwave.
- b. Find the least-squares solution with $x = f(t) = x_0 + v_s t$ through the anchor points. The shockwave speed is then given by v_s and x_0 is nothing more than a spatial intercept. As the linear shockwave may not start with the first vehicle, the first approximation may be a poor one. This can be seen in figures 4a and 4b where the final linear approximation starts around $t = 220$. Therefore the vehicle with the largest error in location between the anchor point and the linear shockwave is excluded and this step is repeated. The stopping criterion is defined as a maximum allowable distance error dependent on the shockwave speed. With larger shockwave speeds, larger distance errors are allowed. Each iteration the distance errors are divided by the latest shockwave speed v_s . This results in a ‘travel time’ for which a maximum error of 8s is the stopping criterion. This value has no meaningful value and was visually confirmed to return the linear part of the shockwave.
- c. The shockwave duration is deduced from the maximum and minimum time of the anchor points of all remaining vehicles. The shockwave range is derived from the duration and shockwave speed. For the shockwave speed the last value of v_s is used.

Table 1 shows the average values of 10 runs for each scenario where each scenario received the same set of random seeds. Note that for average values it may not hold that $v = t/x$. The increase in headway variability appears to have a limited effect on traffic flow stability. From figure 4a and 4b it can however be seen that an increase in headway variability increases the shockwave frequency. Figures 4a and 4b also indicate as expected that the IDM+ shows similar shockwave patterns as the IDM. An increase in CACC2 penetration has large consequences for the

characteristics of shockwaves. The duration is shortened while the range is lengthened. The resulting shockwave speed increases rapidly. This high shockwave speed is visible in figure 4d. The variability between individual runs is larger for 50% CACC2 equipped vehicles than for 0 or 100% CACC2 equipped vehicles. These circumstances are thus less predictable for human drivers.

Figure 4c shows that the AAC algorithm produces a downstream moving shockwave similar to the second shockwave observed in the A270 experiments (figure 2). It is remarkable that the simulation scenario does not reproduce the first upstream wave as with the other algorithms. It should be noted here that the simplified reaction model will

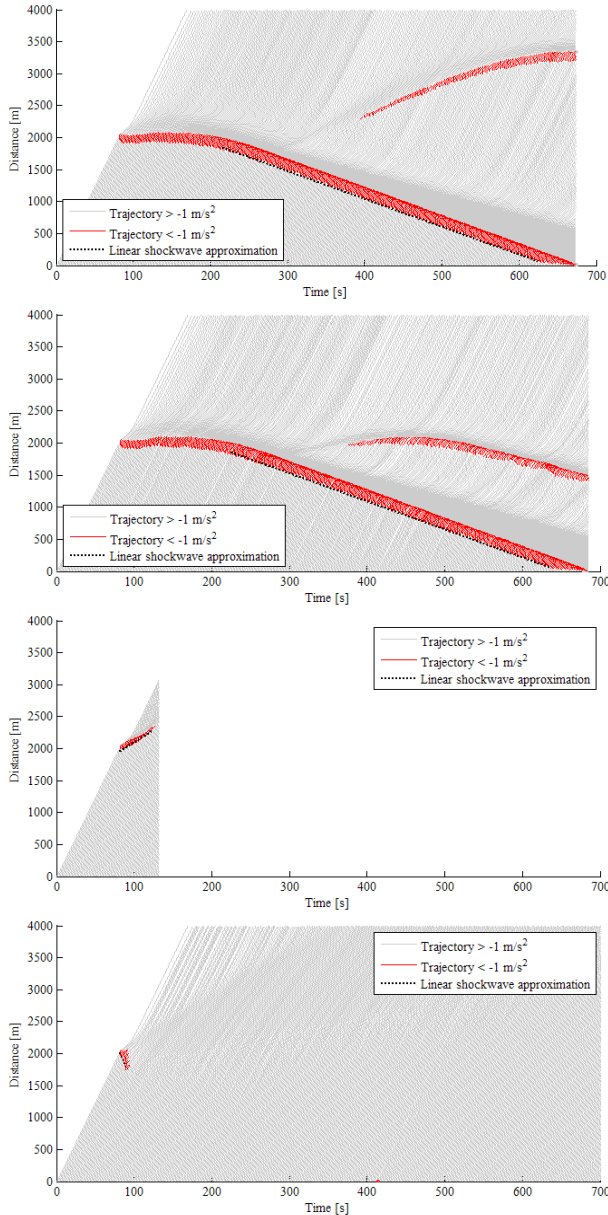


Fig. 4. Shockwave patterns of several scenarios. (a) 0%, headway distribution of 1.2 ± 0.15 s, run 3 (b) 0%, headway distribution of 1.2 ± 0.3 s, run 3 (c) 100% AAC, run 3 (d) 50% CACC2, headway distribution of 1.2 ± 0.15 s, run 3 Only the linear part of the shockwave is considered.

TABLE I
SHOCKWAVE CHARACTERISTICS

algorithm	equipped vehicles	Headway distribution					
		1.2 ± 0.15 s			1.2 ± 0.3 s		
		duration [s]	range [m]	speed [m/s]	duration [s]	range [m]	speed [m/s]
IDM	0%	unstable	unstable	-4,4	unstable	unstable	-4,4
AAC	100%	45,1	341,9	7,6	<i>(without distribution)</i>		
CACC2	50%	9,0	-173,6	-18,7	9,0	-171,1	-18,5
CACC2	100%	7,6	-579,5	-76,6	7,9	-572,2	-73,6

This table gives averages of 10 stochastic runs. Unstable means that the shockwave grows and has a theoretically infinite duration and range. This holds for each of the runs where ‘unstable’ is given.

have a significant effect on wave behavior. Other differences between simulated and field data may come from the variability of headways. For single drivers figure 3 shows large variations while the desired headway is simulated as a constant.

VII. DISCUSSION

Car-following models to date appear unable to capture human driving behavior with realistic traffic flow stability, capacity and reaction time. We have used the IDM+ which shows realistic traffic flow stability but has no reaction time. Given that CACC systems are particularly better than humans at estimation and reaction time, a sensitivity analysis of used reaction times and estimation errors would have been valuable. As a result, our conclusions should be considered explorative. In a qualitative sense our modeling results are similar to the A270 field experiment.

The fast shockwaves of the IRSA controller can be attributed to a summation of (a part of the) interaction terms. As the IRSA controller is sensitive to speed differences only for all but the direct leader, the time step (or system response time) is hardly of influence. Instantaneous acceleration differences need time to result in speed differences. For CACC systems that use acceleration differences the time step will be of influence to the shockwave speed. The value for k_2 is also of influence as this governs the acceleration response and hence acceleration differences. Lower values of k_2 and fewer vehicles that are anticipated for will result in slower shockwaves. Nonetheless these shockwaves will be faster than without CACC2 as any CACC system should anticipate further ahead than humans ($n > n_{human}$ and $k_2 > 0$) to have more stability in traffic flow.

For humans anticipation is an important aspect of driving [14]. Given the larger shockwave speeds of CACC, human drivers may be less able to anticipate and either show more unstable behavior or will increase headways leading to a decrease in capacity relative to a theoretical modeled capacity. In the simulations in this paper we have assumed that drivers still behave as the IDM. Model results of mixed traffic are thus unreliable. Capacity and traffic flow stability may be overestimated. Whether the net effect is positive may

even be disputed for some levels of CACC2 penetration. There may also be serious implications on traffic safety if human drivers do not adapt their method of anticipation or desired headway. Only for a penetration of 100% will these downsides disappear. The results of the AAC algorithm however indicate that using the right CACC algorithm, these implications for human drivers may be small.

Another interesting aspect of human drivers is the interdependency of reaction time and time headway. At merging and diverging sections drivers are faced with short headways and may adjust their reaction time (level of attention) accordingly. This is opposite to the often used notion that drivers will keep a safe distance, depending on their reaction time. A dynamic reaction time might be the key to having collision-free traffic operations with realistic parameter values in car-following models that include a finite reaction time, estimation errors and anticipation while having a realistic macroscopic capacity.

VIII. CONCLUSIONS AND OUTLOOK

We have introduced the IDM+ car-following model which separates the free-flow and interaction term of the IDM. The IDM+ is able to produce realistic capacities with reasonable parameter values.

For the IRSA controller we have found that traffic flow stability improves as shockwaves are quickly damped. This comes at the expense of a larger shockwave range and results in very fast shockwave speeds. This may have undesirable implications on the behavior of human drivers.

The AAC algorithm does not have these implications as the shockwave moves upstream. However, the AAC algorithm is only designed for a penetration rate of 100%. Whether the AAC algorithm is useful in mixed traffic has not been investigated. It however should be (made) applicable for mixed traffic for implementation purposes.

Perturbations in reality may often come from lane changes. In [15] it was even found that all shockwaves at the investigated highway were initiated by lane changes. For a realistic generation of shockwaves a multi-lane facility needs to be modeled. This would also allow for the evaluation of cooperative systems that try to prevent shockwaves not only by speed and headway advice, but also by means of lane advice.

Finally it is noted that there is a lack of data and knowledge on how the longitudinal and lateral driving tasks together produce traffic flow instability. In this article we have looked at the longitudinal driving task with an initial perturbation that may be the result of a cut-in or unstable car-following behavior. Detailed trajectory data of multiple lanes will be required to validate microscopic models of multi-lane facilities.

ACKNOWLEDGMENT

The research reported in this paper was conducted as part of the SPITS project funded by the Dutch Ministry of Economic Affairs, by TomTom, NXP, Logica, TNO, Catena, GreenCat, Task24, Peek, Fourtress, and the universities of Eindhoven, Delft, Twente and Leiden, and the Connected Cruise Control project funded by the Dutch Ministry of Economic Affairs under the High Tech Automotive Systems program, by the universities of Delft, Twente and Eindhoven and NXP, NAVTEQ, TNO, Clifford, Technolution and Rijkswaterstaat.

REFERENCES

- [1] Pueboobpaphan, R., van Arem, B. (2010), "Understanding the relation between driver/vehicle characteristics and platoon/traffic flow stability for the design and assessment of Cooperative Adaptive Cruise Control", Proceedings of the 89th TRB Annual Meeting (upcoming).
- [2] Van den Broek, Th.H.A., Netten B.D., Hoedemaeker M.M., Ploeg J. (2010), "A270 Demo", IEEE ITSC (submitted).
- [3] Treiber, M., Hennecke A., and Helbing D. (2000), "Congested traffic states in empirical observations and microscopic simulations", *Physical Review E*. 62, pp. 1805-1824.
- [4] Bando, M., Hasebe, K., Nakayama, A., Shibata, A., Sugiyama, Y. (1995), "Dynamical model of traffic congestion and numerical simulation", *Physical Review E*. 51, pp. 1035-1042.
- [5] Kesting, A., Treiber, M. (2007), "Calibration of Car-Following Models Using Floating Car Data", *Traffic and Granular Flow '07*, pp. 117-127.
- [6] Helly, W. (1961), "Simulation of bottlenecks in single-lane traffic flow". In: *Theory of Traffic Flow, Proceedings of Symposium on the Theory of Traffic Flow*, pp. 207-238.
- [7] Gipps, P.G. (1981), "A Behavioral Car Following Model for Computer Simulation", *Transportation Research B* 15, pp. 105-111.
- [8] Kesting, A., Treiber, M., Helbing, D. (2010), "Enhanced Intelligent Driver Model to Assess the Impact of Driving Strategies on Traffic Capacity", accepted for publication in the theme issue *Traffic jams - dynamics and control of the Philosophical Transactions of the Royal Society A*.
- [9] Wilmink, I.R., Klunder, G.A., van Arem, B. (2007), "Traffic flow effects of Integrated full-Range Speed Assistance (IRSA)", *Intelligent Vehicles Symposium, 2007 IEEE*, pp. 1204-1210.
- [10] van Arem, B., Driever, H., Feenstra, P., Ploeg, J., Klunder, G., Wilmink, I., Zoutendijk, A., Papp, Z. (2007), "Design and evaluation of an Integrated Full-Range Speed Assistant", *TNO Report 2007-D-R0280/B*.
- [11] van Arem, B., van Driel, C. & Visser, R. (2006), "The impact of cooperative adaptive cruise control on traffic-flow characteristics", *IEEE Transactions on Intelligent Transportation Systems*, 7(4), pp. 429-436.
- [12] van Arem, B., de Vos, A.P., Vanderschuren, M.J.W.A. (1997), "The microscopic traffic simulation model MIXIC 1.3", *TNO Report INRO-VVG 1997-02b*.
- [13] G.J.L. Naus, R.P.A. Vugts, J. Ploeg, M.J.G. van de Molengraft, M. Steinbuch, Cooperative adaptive cruise control, design and experiments, in 2010 American Control Conference; Baltimore, MD, United States, 2010.
- [14] Treiber, M., Kesting, A. & Helbing, D. (2006), "Delays, inaccuracies and anticipation in microscopic traffic models", *Physica A*, 360, pp. 71-88.
- [15] Ahn, S., Cassidy, M.J. (2007), "Freeway traffic oscillations and vehicle lane-change maneuvers", *Proc. 17th International Symposium on Traffic and Transportation Theory, Vol. 1*, pp. 691-710.